Biomaterials Science

Emerging antitumor applications of extracellularly reengineered polymeric nanocarriers

Journal:	*Biomaterials Science*
Manuscript ID:	BM-REV-02-2015-000044.R1
Article Type:	Review Article
Date Submitted by the Author:	13-Mar-2015
Complete List of Authors:	Chen, Jinjin; Changchun Institute of Applied Chemistry, Key Laboratory of Polymer Ecomaterials Ding, Jianxun; Changchun Institute of Applied Chemistry, Key Laboratory of Polymer Ecomaterials Xiao, Chunsheng; Changchun Institute of Applied Chemistry, Zhuang, Xiuli; Changchun Institute of Applied Chemistry, Key Laboratory of Polymer Ecomaterials Chen, Xuesi; Changchun Institute of Applied Chemistry, Chinese Academy of Sciences, Key Laboratory of Polymer Ecomaterials

Biomaterials Science

RSCPublishing

Review

Emerging antitumor applications of extracellularly reengineered polymeric nanocarriers

Cite this: DOI: 10.1039/x0xx00000x

Jinjin Chen,[ab] Jianxun Ding,*[a] Chunsheng Xiao,[a] Xiuli Zhuang[a] and Xuesi Chen*[a]

Received 00th January 2012,
Accepted 00th January 2012

DOI: 10.1039/x0xx00000x

www.rsc.org/

Recently, the polymeric nanocarriers with shielding surfaces, *e.g.*, poly(ethylene glycol) and small molecules, have been widely applied in antitumor drug delivery mainly because of their stealthy during blood circulation. However, the shielding shell greatly hinders the tumor penetration, drug release, and cell internalization of the nanocarriers, which leads to the unsatisfactory therapeutic efficacy. To integrate the extended blood circulation time and the enhanced drug transmission in one platform, some extracellularly stimuli-mediated shell-sheddable polymeric nanocarriers have been exploited. The systems are stealth and stable during blood circulation, as soon as they reach the tumor tissue, the shielding matrices are removed triggered by the extracellular endogenous stimuli (*e.g.*, pH and enzyme) and exogenous excitations (*e.g.*, light and voltage). This review mainly focuses on the recent advances of the designs and emerging antitumor applications of the extracellularly reengineered polymeric nanocarriers for directional drug delivery, as well as the perspectives for future developments.

1 Introduction

An important requirement to the systemic intravenous application of the polymeric nanocarriers of antitumor drugs is the ability to circulate in the bloodstream for a prolonged period of time. To achieve this, many shielding processes have been carried out on the surface of nanocarriers, such as PEGylation[1] and small molecule cage.[2] Poly(ethylene glycol) (PEG), a mostly applied shielding material that can be easily decorated to nanocarriers through covalent linkages or non-covalent interactions, can reduce both opsonization by proteins and uptake by mononuclear phagocytes.[3] Additionally, the nanocarriers with nonspecific cations or specific tumor targeting ligands are caged with small molecules to reduce their interactions with the cells during blood circulation or in normal tissues.[4,5] The shielded nanocarriers are proved to be stealth during blood circulation and can accumulate at tumor site through passive or active targeting.[6–8] On the other hand, the drugs loaded in the nanocarriers are also stabilized by the shielding shell.[9]

Although more drug-loaded nanocarriers can safely arrive at the lesion site due to the shielding surface, the further drug release and/or cell internalization are greatly hindered because of PEG and the inactivated small molecules.[10] To integrate the improved blood stability, and the enhanced drug release and/or cell uptake, a kind of extracellularly reengineered nanocarriers triggered by the tumor extracellular stimuli have been exploited.[11–13] In these platforms, the tumor extracellular stimuli-responsive linkages or interactions have been introduced to the nanocarriers.[14–16] The sheddable shells always exhibit the PEGylation to dePEGylation,[17,18] negative to positive charge,[19,20] or caged to uncaged ligand transitions,[21] which are triggered by either the endogenous stimuli (*e.g.*, pH and enzyme) or exogenous ones (*e.g.*, light and voltage) (Scheme 1). After the shedding of shell, there are two pathways for the drugs to be delivered into the cells: (i) diffusion of the extracellularly released drugs into tumor cells after the deshielding of nanocarriers; (ii) internalization of complete nanocarriers into tumor cells through the enhanced endocytosis mediated by the exposed cations or ligands. The two mechanisms all promote the drug absorption by tumor cells because the small molecule drugs more easily pass cell membranes than larger nanocarriers, and the exposed cations or ligands on the surface enhance the cell uptake of the reengineered nanocarriers.[22] Compared to the shell-unsheddable nanocarriers, the tumor extracellularly reengineered nanocarriers are considered to be more efficient to the directional drug delivery.[5,23,24] This review highlights the recent progress in the tumor extracellularly reengineered polymeric nanocarriers for smart drug delivery and shows the perspectives for further potential advances.

2 DePEGylation-related shell-shedding

As mentioned above, PEGylation is the most commonly used shielding approach because PEG can not only improve the solubility but also resist the adsorption of proteins, which all prolong the blood circulation time of nanocarriers.[3,5,25] The PEG coating can be introduced into the surface of nanocarrier through the covalent linkages or non-covalent interactions. Both the linkages and interactions can been removed under extracellular stimuli in the shell-sheddable nanocarriers.

The stimuli-sensitively cleavable covalent linkages are widely used in the polymeric nanoparticles for drug delivery, mainly because of the stability of nanovehicles under normal physiological

condition and specific drug release under stimuli.[26] In details, the dePEGylation is easily realized through the cleavage of covalent linkages under the tumor extracellular microenvironment, such as pH and enzyme,[26,27] and external stimuli, such as light[28–31] and voltage.[32] In addition, the non-covalent interactions, *e.g.*, electrostatic, host-guest, hydrogen bonding, stereocomplex, and coordination interactions, have been extensively investigated in the field of controlled drug delivery because they are facile and mostly reversible.[16] Among all these non-covalent interactions, the dePEGylation based on the reduction of electrostatic interaction can be easily realized because the electrostatic interaction can be weakened by the protonation[33] or charge reversal[34] in the tumor extracellular acidic condition. Moreover, there is a series of stimuli-responsive host-guest interactions that have been reported.[35] The separation of the host-guest interactions mainly results from the changes of the stereo structure[36] and the hydrophobic-hydrophilic transition[37] under stimuli. These reengineered polymeric nanocarriers based on the approach of dePEGylation integrate the blood stability and the tumor reactivation through the mediation of tumor extracellular stimuli, which show great superiority compared with the PEG-unsheddable ones.

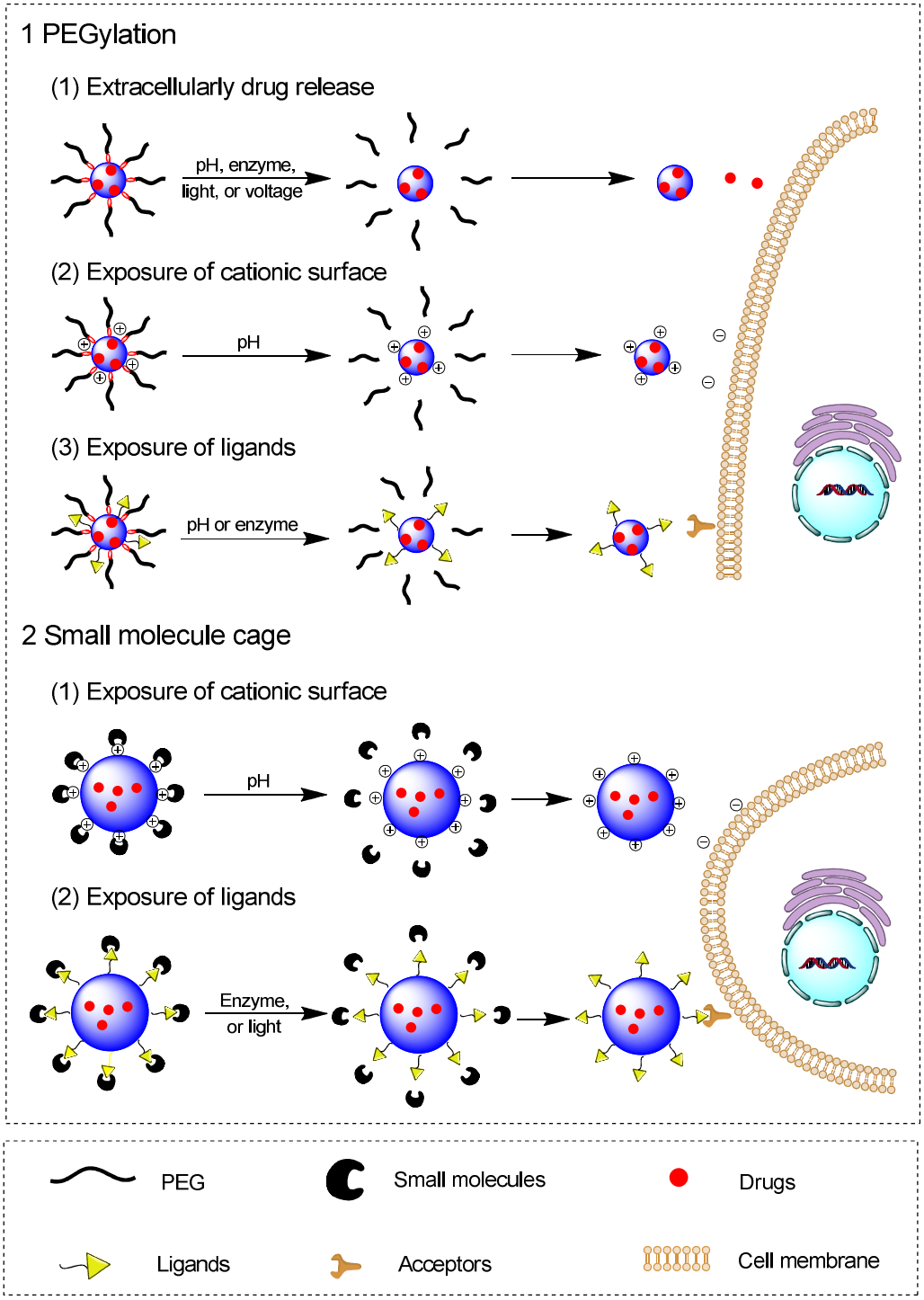

Scheme 1 Schematic diagram of various types of extracellularly reengineering processes under endogenous or exogenous stimuli.

2.1 pH-triggered extracellular dePEGylation

Among all the extracellular stimuli, pH is the most generally and frequently used one because of the universality of the acidic microenvironment in various types of solid tumors. In fact, the tumor extracellular pH (*i.e.*, 6.5 – 7.2) is slightly lower than that of blood (*i.e.*, ~7.4), and the intracellular pH is even lower (*i.e.*, 4.0 – 6.5).[38–40] Up to now, most of the pH-induced dePEGylation focus on the intracellular microenvironment because various pH-sensitive linkages are responsive to lower intracellular acidic condition. However, the extracellular pH-triggered dePEGylation is more meaningful for drug delivery ascribed to the solution of the low affinity of the PEG coated-nanocarriers to cell membrane. The most frequently reported mild extracellular acid-sensitive linkages include imine[17] and amide with neighboring carboxyl group.[41] The shedding of PEG leads to the disassembly of nanocarriers and/or further accelerates the drug release. There are also many PEGylated nanocarriers assembled through electrostatic interaction. They always consist of an anionic PEG shell and a cationic core, and the surface potential is usually adjusted to be neutral or negatively charged to improve the stability in blood.[16] After accumulating at the tumor site, PEG was detached through two approaches under the extracellular pH (*i.e.*, ~6.8). One way is the acid-triggered protonation of the negative group[33] and another is the charge reversal activated by the acid-cleavable linkage.[34] As a result, the exposed cationic core can greatly enhance the internalization into the tumor cells and finally gain an improved antitumor efficacy.

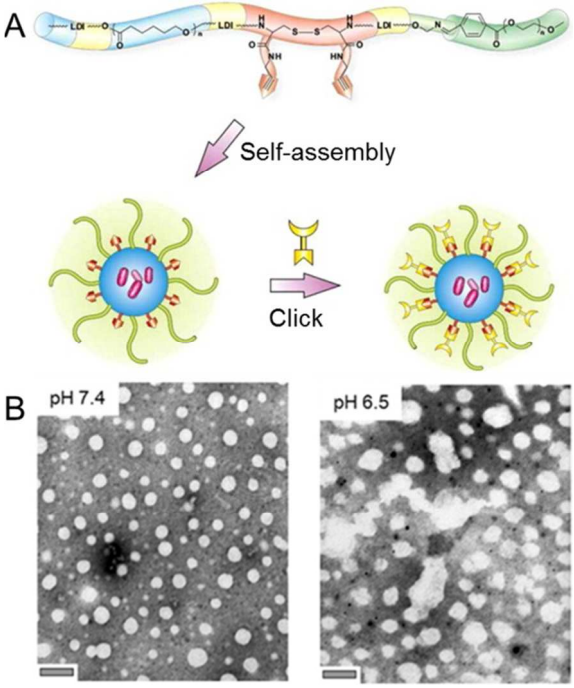

Fig. 1 (A) Structure of benzoic imine-linked diblock polymer; (B) TEM microimages of self-assemblies of cleavable PEGylated diblock copolymer at pH 7.4 and 6.5. The scale bars indicate 100 nm.[43]

In Qu and Yang's group, a liner benzoic imine-linked diblock polymer was simply prepared by the reaction between the benzaldehyde-terminated methoxy poly(ethylene glycol) (mPEG) and *n*-octadecane amine.[42] The copolymer spontaneously self-assembled into micelle with an average diameter of 181 nm determined by dynamic laser scattering (DLS), and the size was 183 nm at pH 6.5, which was almost the same as that at pH 7.4. Moreover, a sharp increase of zeta potential from 0 to 30 mV was observed as the decrease of pH from 7.4 to 6.5 ascribed to the detachment of PEG producing the positively charged octadecane amine (p*K*a ~11). The doxorubicin (DOX)-loaded micelle with drug loading content (DLC) and diameter at 30.0 wt.% and 216 nm, respectively, was obtained through a solvent evaporation method. The PEG-sheddable micelle showed the accelerated drug release behavior and enhanced cell uptake of DOX at pH 6.8 compared with the PEG-unsheddable one, which revealed that the shell-shedding can greatly improve the extracellular release and cell uptake of drug. The PEG-cleavable polyurethane micelles based on the pH-sensitive benzoic imine were prepared in Tan's group for the multifunctional delivery of antitumor drug.[43] As shown in Fig. 1A, the polyurethanes with different components were synthesized through the condensation reaction among the L-lysine ethyl ester diisocyanate (LDI)-modified poly(ε-caprolactone) (PCL), alkynyl-decorated L-cystine derivative (Cys-PA), and benzoic imine-decorated mPEG (BPEG). The hydrodynamic diameters (D_hs) of the above polyurethane micelles were in the range of 67.3 – 153.0 nm determined by DLS. The nanocarrier was stable at pH 7.4 while became larger moderately at pH 6.5. It was because that the benzoic imine bond was cleaved under acidic condition, which led to the partial shedding of PEG and the further aggregation of micelle (Fig. 1B). DOX was loaded into the micelle through nanoprecipitation technique with DLC of over 23 wt.%, and then folic acid (FA) was conjugated to the Cys-PA block through "click" chemistry. The shell-sheddable polyurethane micelle could target to the FA-receptor positive HeLa cells (a human cervical carcinoma cell line), resulting in the enhanced cell internalization and increased antitumor efficacy compared with the non-targeted one. Furthermore, a core-shell nanocarrier was reported by Qu, Yang, and coworkers.[17] It was formed by a cationic cholic acid-grafted poly(L-lysine) core (PLL-CA) and a benzaldehyde-terminated mPEG shell. The diameters of the aggregates were found in a range of 160 – 270 nm at pH 7.4 by DLS. The zeta-potentials of the shell-sheddable polycationic nanoparticles were strongly pH-dependent in a range covering the normal physiological pH (*i.e.*, ~7.4), extracellular pH (*i.e.*, 6.8), and intracellular pH (*i.e.*, 5.0 – 6.0), which were upregulated by the decrease of pH. The micelle showed better biocompatibility at normal physiological pH due to the PEGylation. The cell viability of the PEG-coated PLL-CA (IC_{50} = 0.124 mg mL^{-1}) was much higher than that of the uncoated PLL-CA (IC_{50} = 0.0326 mg mL^{-1}). Moreover, it became membrane disruptive to porcine erythrocytes used as the model of a biological membrane at pH 6.0 compared with that at pH 7.4, which proved that the exposed cationic surface could enhance the affinity of nanocarrier to the cells.

Another kind of mild pH-sensitive micelle based on *cis*-aconityl linkage was carried out in Du's group.[26] mPEG was decorated to the cationic surface of the stearic acid-grafted chitosan through sequential ring-opening and condensation reactions. The D_h of the shielded micelle was determined to be 50.6 ± 7.0 nm, which was larger than that of the unshielded one (*i.e.*, 27.6 ± 1.8 nm). The zeta potential of the micelle was also decreased from 39.7 ± 1.6 to 24.8 ± 5.5 mV after shielding process. DOX was chosen as a model drug, and the DLC and drug loading efficiency (DLE) of the micelle were 87.59 ± 2.76 and 4.19 ± 0.13 wt.%, respectively. The pH-triggered dePEGylation was demonstrated to enhance the internalization into tumor cells, not only for the positively charged vehicles but also for the encapsulated DOX. Furthermore, the *in vivo* studies indicated that the acid-triggered shell-sheddable DOX-loaded micelle conducted well in inhibiting the growth of the human hepatoma BEL-7402 tumor xenografted in male BALB/C nude mouse while reducing the toxicity on the body. Overall, the results suggested that the above smart micelle was a promising candidate for controlled drug delivery.

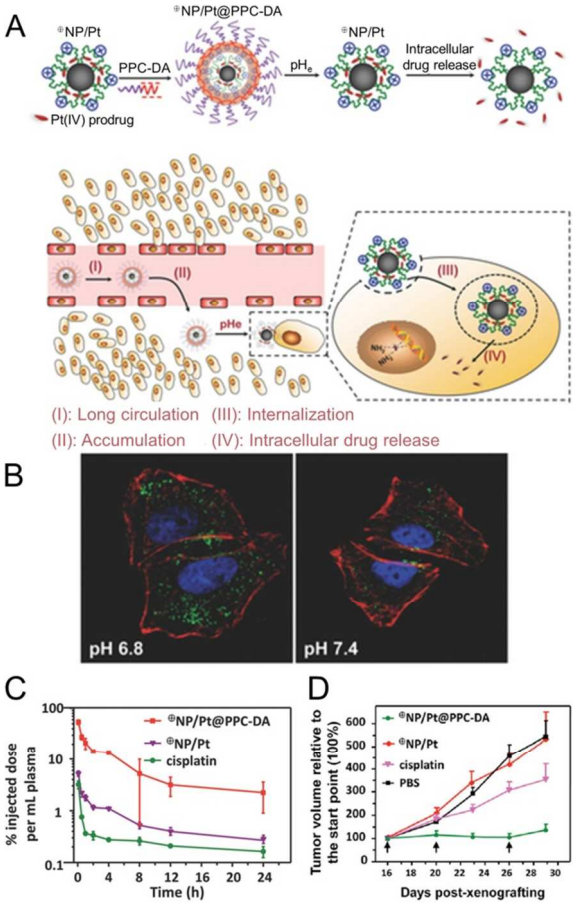

Fig. 2 (A) Schematic illustration of preparation of ⊕NP/Pt@PPC-DA nanocarrier and process of extracellularly reengineering. (B) Internalization of FITC-labeled ⊕NP/Pt@PPC-DA by A549R cells observed through confocal laser scanning microscopy (CLSM). Cells were cultured with nanocarrier (green) at different pHs for 2 h. Cell cytoskeleton F-actin was stained with Alexa Fluor 568 phalloidin (red) and cell nucleus was stained with DAPI (blue). (C) Plasma platinum concentrations at different times after intravenous injection of various formulations. (D) Inhibition of tumor growth in a murine tumor model with A549R tumor xenograft after treatment with different formulations.[34]

The origin research of the electrostatic interaction-mediated reversibly PEGylated polymeric nanocarrier was carried out by Bae and his coworkers.[33] The nanocarrier was composed of the negatively charged shielding layer of poly(ethylene glycol)-*block*-poly(methacyloyl sulfadimethoxine) (PEG-*b*-PSD) and TAT peptide-terminated poly(ethylene glycol)-*block*-poly(L-lactide) (TAT-PEG-*b*-PLLA) micelle. TAT peptide is a kind of cell-penetrating peptide (CPP) which can greatly enhance the cell uptake of the nanocarriers. But the TAT peptide-modified nanocarriers are not stable during the blood circulation because it has no specificity toward normal and tumor cells. The size of the shielded nanocarrier was in the range of 60 – 90 nm between pH 8.0 and 6.8. However, two populations were observed between 6.6 and 6.0, one about 40 nm in size corresponding to the TAT-PEG-*b*-PLLA micelle and the other about 200 nm attributed to the aggregated hydrophobic PEG-*b*-PSD. The result proved the reengineering process of the nanocarrier. The nanocarrier was adjusted to be neutral under the conditions of pH higher than 6.8 (~0 mV), while it rapidly turned to be positively charged when the pH decreased below 6.6 (over 4 mV), which resulted from the protonation of sulfonamide group. It was demonstrated that the shell-sheddable micelle could be more efficiently internalized into MCF-7 cells (a human breast carcinoma cell line) at pH 6.6 than that at pH 7.4. Recently, another extracellularly pH-sensitive shell-sheddable nanocarrier was exploited in the same group.[44] Similarly, PEG-*b*-PSD was used as the shielding shell. The poly(L-histidine)-*block*-short branched polyethyleneimine (PLH-*b*-sbPEI) assembled into the cationic core with a D_h of ~34 nm. After coating of PEG-*b*-PSD onto the core, the D_h of the nanocarrier increased to around 50 nm. The zeta potential of the micelle increased from –10.8 to 43 mV after the shielding process. As the pH decreased to 6.6, the cell uptake of the Cy3-labeled PLH-*b*-sbPEI to MCF-7 cells was greatly enhanced. Paclitaxel (PTX) was loaded into the nanocarrier as a model drug. Typically, the unshielded PTX-loaded micelle with DLC of 7.5 wt.% was about 40 nm in diameter, while the size of the shielded nanocarrier increased to about 65 nm. Toward the MCF-7 tumor-xenografted female BALB/c nude mouse model, the PEG-shielded paclitaxel (PTX)-loaded nanoparticle exhibited excellent tumor inhibition compared with free PTX and the nanoparticle without PEG coating.

The dePEGylation based on the charge reversal approach was investigated in Wang's group.[34] As shown in Fig. 2A, the amphiphilic block copolymer of poly(ε-caprolactone)-*block*-poly(2-aminoethylethylene phosphate) (PCL-*b*-PAEEP) was prepared to be the cationic core with a zeta potential of 38.7 mV, and then the carboxylated Pt(IV) prodrug was conjugated to it *via* condensation reaction, yielding ⊕NP/Pt. The platinum content of ⊕NP/Pt was 8.41 wt.%. Finally, the 2,3-dimethylmaleic anhydride (DMMA)-modified methoxy poly(ethylene glycol)-*block*-poly(allyl ethylene phosphate) (mPEG-*b*-PAEP) (*i.e.*, PPC-DA) was mixed with the core to form the negatively charged (–30 mV) and pH-dependent shell-sheddable nanocarrier (*i.e.*, ⊕NP/Pt@PPC-DA). ⊕NP/Pt@PPC-DA exhibited a slightly increased D_h (44.5 nm) compared with that of ⊕NP/Pt (31.5 nm). After the pH-mediated dePEGylation, the positively charged ⊕NP/Pt was exposed and hence gained the promoted internalization to the cisplatin-resistant A549R cells (a human lung carcinoma cell line) at pH 6.8 *in vitro* (Fig. 2B). The shell-sheddable nanocarrier exhibited prolonged blood circulation compared with free drug and ⊕NP/Pt (Fig. 2C). As a result, the efficient inhibition of tumor growth was observed in a male BALB/c nude mouse model bearing A549R xenograft (Fig. 2D).

2.2 Enzyme-mediated extracellular dePEGylation

The upregulation of certain enzymes in the intratumoral microenvironment can be significant. For example, matrix metalloproteinases (MMPs), particularly gelatinases A and B (*i.e.*, MMP-2 and MMP-9), play an important role in the angiogenesis, invasion, and metastasis of tumor cells.[45,46] Due to the rapid proliferation of tumor, MMPs overexpress in extracellular matrix. Benefiting from it, lots of enzyme-sensitive vehicles have been explored for tumor targeting drug delivery.[46]

Liu and coworkers synthesized a diblock copolymer, *i.e.*, PEG-Pep-PCL, which was linked with a gelatinases (MMP-2/9, type IV collagenases) cleavable peptide.[47] Docetaxel (DTX) was loaded into the micelle formed by PEG-Pep-PCL to improve the radiotherapy efficacy. The average diameter of the DTX-loaded micelle was about 85 nm, which could enhance the accumulation in tumor tissue through the EPR effect. The DLC was 20.3 wt.%, and the DLE was high to 80.7 wt.%. Coumarin-6 was used as a fluorescent cargo to evaluate the efficiency of drug uptake by cells. In high gelatinases-expressed BGC823 cells (a human gastric carcinoma cell line), more cell uptake of the coumarin-6-loaded nanocarrier occurred compared with that toward the low gelatinases-expressed GES-1 cells (a

human gastric epithelial cell line), which proved that the enzyme-sensitive dePEGylation could increase the release of the loaded cargo. Additionally, the shell-sheddable nanocarrier could enhance the radiotherapy efficacy. The intracellular reactive oxygen species (ROS) level of the free DTX- and DTX-loaded nanoparticle-treated BGC823 cells after radiation were upregulated by 1.14- and 1.41-fold compared with the group treated with radiation only, respectively.

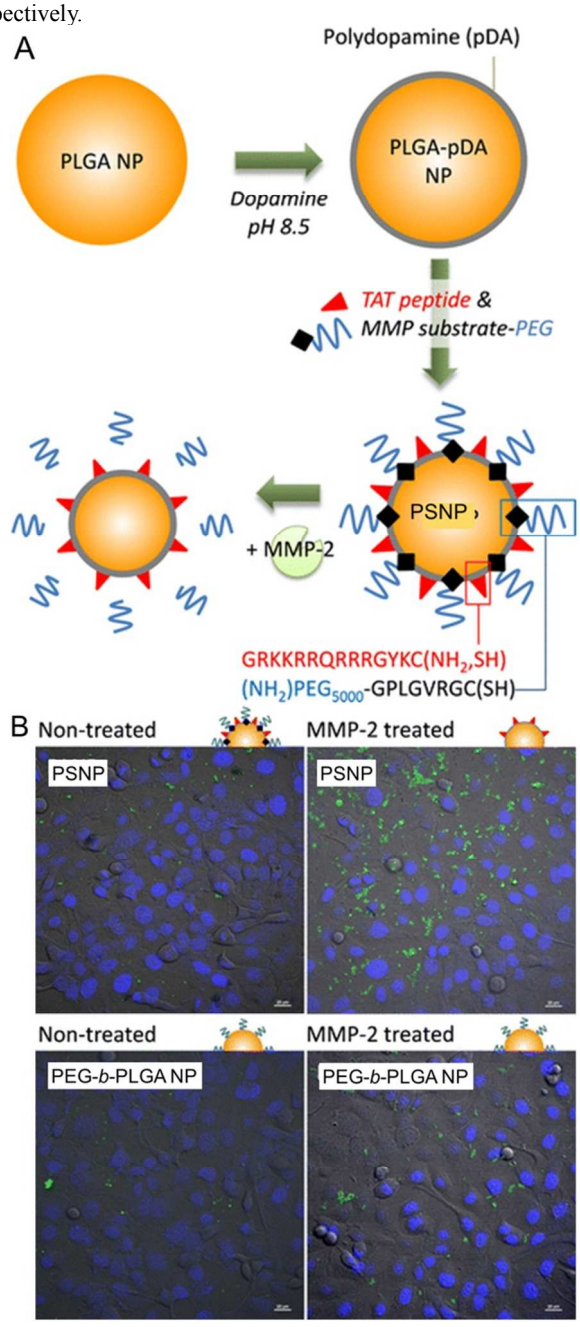

Fig. 3 (A) Schematic diagram of preparation of extracellular PSNP; (B) Cell uptake of PSNP and PEG-*b*-PLGA nanoparticle (NP). Nanoparticles were added to SKOV-3 cells in culture medium supplemented with 10% (V/V) FBS. Nanoparticle was labeled with fluoresceinamine (green), and nucleus was stained with DRAQ5 (blue).[48]

Another MMPs-triggered shell-sheddable nanocarrier was reported by Yeo's group.[48] Typically, the polydopamine-coated poly(lactide-*co*-glycolide) (PLGA) nanoparticle was further modified with TAT peptide (PLGA-pDA-TAT) only or dual-modified with TAT peptide and PEG-MMP-substrate peptide as shown in Fig. 3A. In this work, the TAT peptide was "hided" under protective PEG layer at the normal physiological condition. When it arrived at the tumor extracellular microenvironment with the overexpressed MMP-2, the protective PEG was detached due to the cleavage of the MMP-2-sensitive linkage, which further contributed to the promoted internalization of nanocarrier. PTX was loaded into the PEG-sheddable nanoparticle (PSNP) with DLC of 20.0 wt.%. The PTX-loaded PSNP had an increased D_h of 210.8 ± 37.9 nm compared with that without PTX. The MMP-2-pretreated PSNP showed relatively improved cell uptake of SKOV-3 cells compared to the MMP-2-non-treated one and nanoparticle with non-cleavable PEG, as shown in Fig. 3B.

As mentioned above, MMPs are a kind of commonly distributed enzyme in almost every type of human malignancies.[45] Apart from them, there are some specifically overexpressed enzymes, such as aminotransferase, trypsin, azoreductase, pepsin, and so on, that can be applied as the target sites for the treatment of specific tumors.[27] Azoreductase, which can cleave the azo-based linkage, is produced by the microbial flora in human colon. Khan's group recently developed the azobenzene-linked poly(ethylene glycol)-*block*-polystyrene (PEG-N=N-PS) amphiphilic copolymer.[27] The copolymer could self-assemble into micelle with D_h of 65 nm in aqueous solution. The micelle had regular spherical shape but disassembled after being treated with azoreductase, which revealed good enzyme-sensitive disassemble of micelle and great potential in colon-specific drug delivery.

2.3 Light-induced dePEGylation

Light is an external stimulus and can control the release of a drug at the desired time and site, which benefits to targeting drug delivery in malignancy treatment. Moreover, the wavelength, intensity, period, and acting position of light can all be controlled. The light-triggered dePEGylation processes through the cleavage of the photo-sensitive linkages have already been reported.[49–52] The light-induced reengineered nanocarriers are usually formed by a hydrophilic PEG shell and a hydrophobic core, and the linkage of the two blocks are light-cleavable, such as *o*-nitrobenzyl ester[28,29,31] and truxillic acid derivatives.[30]

Burdick's group firstly synthesized the *o*-nitrobenzyl (ONB)-linked copolymer of poly(ethylene glycol)-*o*-nitrobenzyl-poly(ε-caprolactone) (PEG-ONB-PCL) through condensation reaction of 2-nitrophenylalanine-modified PEG and carboxy-terminated PCL.[28] The diblock polymer could self-assemble into vesicle with the diameter at around 200 nm determined by cryogenic transmission electron microscopy (cryo-TEM). The eluted PEG peak in the gel permeation chromatography (GPC) of the ultraviolet (UV)-exposed vesicle increased with the extension of irradiation time (λ = 365 nm). The result proved the excellent photo-sensitivity of the block copolymer. Furthermore, the ONB-linked block copolymer of poly(ethylene glycol)-*o*-nitrobenzyl-polystyrene (PEG-ONB-PS) was synthesized *via* the atom transfer radical polymerization (ATRP) using PEG-ONB-Br as an initiator in Fustin's group.[29] The light-induced cleavage of OBN in PEG-OBN-PS was monitored by ultraviolet-visible (UV-vis) spectrophotometer. As the irradiation time increased (λ = 300 nm), the absorption at 308 nm decreased significantly, which revealed the destruction of the ONB linkage. Another light-sensitive block copolymer using the truxillic acid derivative as the junction was prepared by Keller and coworkers.[30] The copolymer was also synthesized by the ATRP polymerization. The required UV wavelength for the photocleavage of this copolymer was short (λ < 260 nm), which was different from the ONB linkage. The difference of the photo-sensitivity might have

great potential for the development of the multi-photosensitive polymers, which could be selectively reengineered in specific blocks through the irradiation of the lights with different wavelengths.

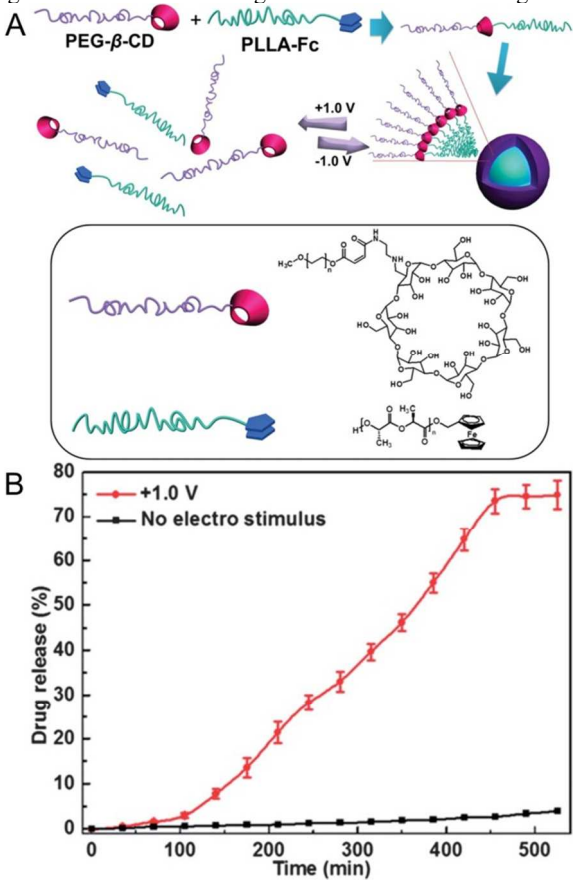

Fig. 4 (A) Scheme of voltage-controlled assembly and disassembly of PEG-β-CD/PLLA-Fc micelle; (B) Release behavior of PTX-loaded polymeric micelle with or without +1.0 V stimulus.[32]

2.4 DePEGylation through elimination of host-guest interaction

The host-guest interaction based on macrocyclic molecules is a very important linkage that has been extensively investigated in fabricating the platforms of drug delivery.[35] The stimuli-responsive host-guest interactions have been widely reported,[36] while the shell-sheddable polymeric nanocarriers based on them were seldom reported.

As a representative example, a family of voltage-sensitive ferrocene-based supramolecular nanoparticles was explored, and some of them have been applied in controlled drug delivery through the shell-shedding process.[37,53–55] As depicted in Fig. 4A, a voltage-sensitive reengineered micelle was prepared in Yuan's group, which was composed of the β-cyclodextrin (β-CD)-modified poly(ethylene glycol) (PEG-β-CD) and ferrocene-functionalized poly(L-lactide) (PLLA-Fc).[32] The two polymers could self-assemble into stable micelle with D_h at about 150 nm in aqueous solution mediated by the host-guest interaction between β-CD and Fc. The smart micelle showed voltage-controlled assembly-disassembly transition and drug release (Fig. 4B). The reversible property endowed the voltage-sensitive micelle with great potential as a site-specific drug delivery system.

3 Nanoparticle reengineering mediated by uncaging small molecules

Although dePEGylation is the mostly used shell-shedding approach, the small molecules have also been applied in the reengineering of the dormant cations or ligands. The cations or ligands on the surface of nanocarriers are proved to induce enhanced cell internalization.[22] However, the applications of above modifications are limited because the non-specificities of cations and some ligands (*e.g.*, CPPs and FA) result in serious adsorption by proteins or clearance by monocytes in blood.[4,56] Therefore, small molecule cages are used as a usual approach to shield the cations or ligands.[57–59] When the nanocarriers accumulate at the tumor site, the small molecules are removed triggered by both the internal and external stimuli. Subsequently, the cation- or ligand-modified surfaces are exposed and reactivated, which can further improve the cell uptake of nanocarriers.

3.1 Intratumoral acidity-activated charge-reversal transition

Amides with β-carboxylic acid groups are proved to have different levels of acid-sensitivity and have been applied to shield the cationic amino groups on the surface of nanocarriers.[41] The cleavage of those amides results in the charge-reversal of nanocarriers and further leads to the enhanced cell uptakes of the reengineered nanoparticles. Therefore, these types of amides have been widely employed in various smart nanocarriers with the intratumoral transition from negative to positive charge.[12,58,60]

Shen and coworkers firstly used the *cis*-1,2-cyclohexanedicarboxylic anhydride (CHDA) to cage the primary and secondary amines of the micelle self-assembled from poly(ε-caprolactone)-*block*-short branched polyethyleneimine (PCL-*b*-sbPEI) to form the charge-reversal nanoparticle (PCL-*b*-sbPEI/CHDA).[20] PCL-PEI/CHDA was negatively charged at physiology condition (~–20 mV at pH 7.4) but quickly became positively charged at pH 6 (~8 mV), which indicated the successful reengineering of nanoparticle. Then, FA was conjugated to the surface of the nanoparticle to improve the tumor targeting property, and DOX was loaded into the nanoparticle with DLC and diameter at 14.6 wt.% and about 120 nm, respectively. The cells cultured with the DOX-loaded nanocarrier at pH 6.0 exhibited significantly higher fluorescence intensity than that cultured with free DOX. This DOX-loaded nanocarrier also showed enhanced inhibition against SKOV-3 cancer cells than that of free DOX *in vitro*. In Wang's group, another kind of anhydride named DMMA was applied for the tumor extracellularly reengineered nanocarrier.[19] The nanogel of poly(2-aminoethyl methacrylate hydrochloride) (PAMA) was prepared through inverse microemulsion polymerization using poly(ethylene glycol) diacrylate (PEGDA) as a crosslinker and potassium persulfate as an initiator. Then the amino groups on the surface of nanogel were caged with DMMA or succinic anhydride (SA) to obtain the charge-reversal nanogel (PAMA-DMMA) or non-charge-reversal one (PAMA-SA). PAMA-DMMA and PAMA-SA exhibited the negative zeta potentials at –17 and –25 mV, respectively, and well-distributed D_h of both ~100 nm. PAMA-DMMA changed from negative to positive charge at acidic tumor extracellular microenvironment (*i.e.*, pH ~6.8) within 1 h resulting from the cleavage of amide bond. The nanogel was distributed in the cytoplasm of MDA-MB-435s cells (a human breast carcinoma cell line) after the incubation with fluorescein isothiocyanate (FITC)-labeled PAMA-DMMA at pH 6.8, while it seemed to attach to the cell membrane at pH 7.4. The results revealed the efficient pH-mediated reengineering of nanocarrier. DOX was loaded into both negatively charged PAMA–DMMA and PAMA–SA with extremely high DLE of 94.9 and 98.7 wt.%, respectively, in comparison with that of positively charged PAMA nanogel (18.6 wt.%). The proliferation inhibition efficacy of the DOX-loaded PAMA-DMMA nanogel against MDA-MB-435s cells was better even than that of

free DOX at pH 6.8. It demonstrated that the reengineering process enhanced the cell uptake of nanogel, which led to the significantly promoted efficiency in the inhibition of tumor cell proliferation.

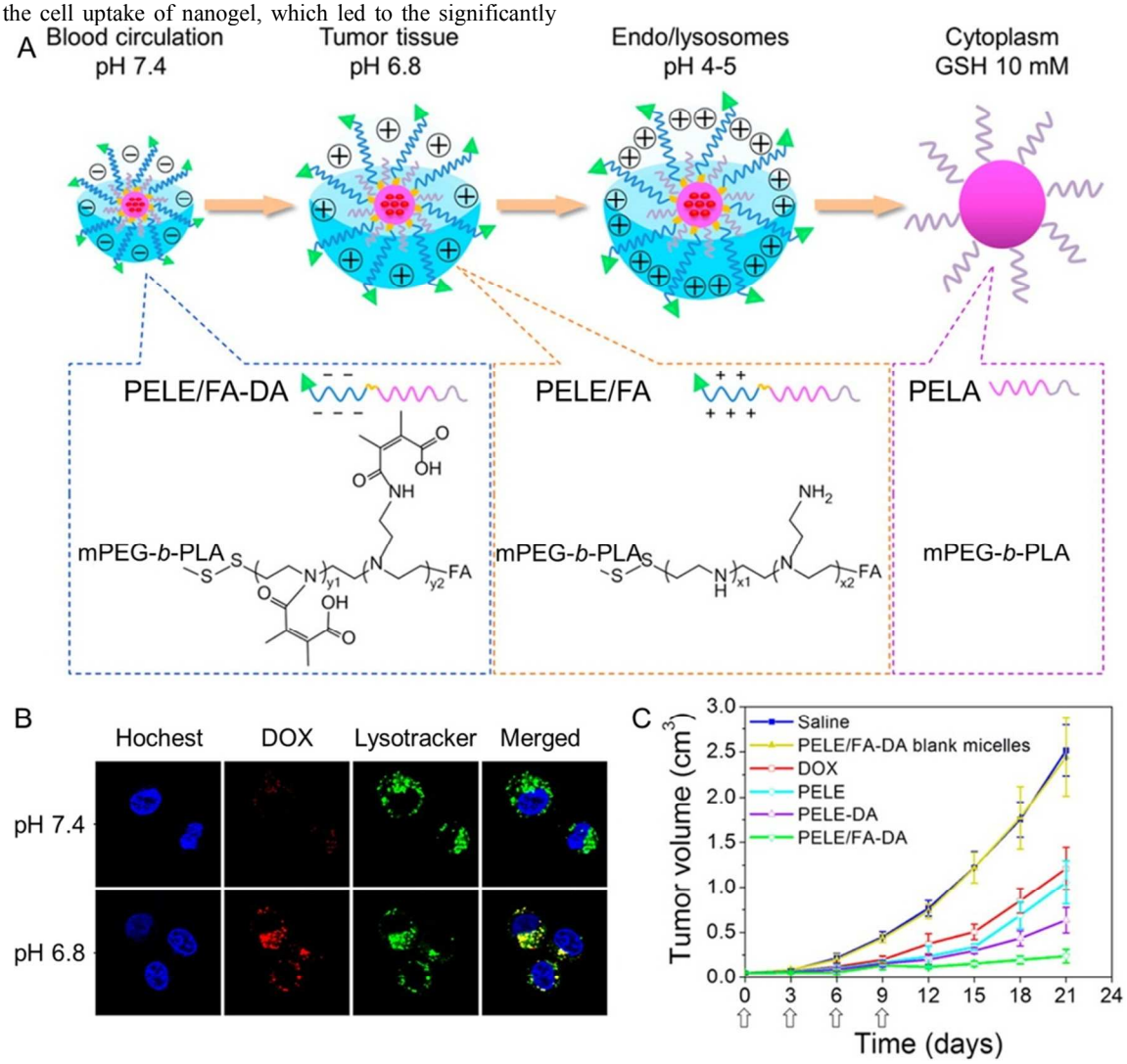

Fig. 5 (A) Schematic design of targeted micelle (PELE/FA-DA) with extracellularly reengineering property in tumor tissue and intracellularly GSH-triggered drug release. (B) Cell uptake of DOX-loaded PELE-DA micelle at pH 7.4 or 6.8 after incubation with HeLa cells for 1 h. Nucleus was stained with Hoechst 33342 (blue) and lysosome was stained with Lysotracker (green). (C) Tumor growth inhibition of 4T1 tumor in BALB/c mice after tail vein injection of different formulations (n = 7).[61]

As the development of intelligent nanocarriers, the multi-responsive ones that developed for the programmed drug delivery exhibited great advantages compared to the traditional single stimulus-responsive drug delivery systems.[10,11] This kind of nanocarriers could firstly response to the extracellular microenvironment for the reengineering processes and then obtained triggered drug release under the intracellular condition. For example, Wang and colleagues prepared a shell-sheddable nanocarrier for the programmed drug delivery.[60] mPEG-*b*-PAEP was firstly conjugated with DOX through an acid-labile hydrazone bond, and then the remaining amino groups were partly caged with DMMA to get the negatively charged nanocarrier (PPC-Hyd-DOX-DMMA). The nanoparticle with the DOX content of 8.32 wt.% was ~27 nm in diameter determined by DLS. Due to the different pH-sensitivities of the amide and hydrazone bonds, the DMMA cage firstly left at the extracellular pH. The negatively charged surface turned to be positively charged at pH 6.8 in about 20 min, which enhanced the cell internalization of micelle. Finally, the hydrazone bond was broken in the intracellular critical acidic microenvironment, and DOX was released to the nucleus quickly. The prodrug micelle exhibited the excellent property of programmed drug delivery. The fluorescence intensity of DOX in PPC-Hyd-DOX-DMMA-treated MDA-MB-231 breast carcinoma cells at pH 6.8 was stronger than that at pH 7.4, which revealed that the excellent extracellularly reengineering property enhanced the cell uptake of the formulation. DOX distributed from lysosome to nucleus as the time increasing from 1 to 12 h, which indicated the enhanced DOX release resulting from the rupture of hydrazone bond under the severe acidic intracellular microenvironment. Similarly, as shown in Fig. 5A, another pH and reduction dual-sensitive programmed nanocarriers was prepared in Zhou's group by the self-assembly of the DMMA-caged, FA-modified, and disulfide bond-linked copolymer of mPEG-*b*-PLA-S–S-sbPEI/FA-DMMA (*i.e.*, PELE/FA-DA).[61] The D_h of the nanocarrier was determined to be ~90 nm, while it changed to ~300 nm after the treatment with 10.0 mM GSH for 2 h. In addition, the platform represented an ultrasensitive charge reversal from ~–13 mV to ~15 mV after the incubation at extracellular acidity of pH 6.8 for about 1 h, and could be significantly internalized by malignant cells.

Subsequently, the sbPEI block was detached triggered by the intracellular GSH at a high concentration, and DOX was finally released to the nucleus. The cell uptake of the DOX-loaded PELE-DA micelle at pH 6.8 after incubation with HeLa cells for 1 h was much higher than that at pH 7.4 (Fig. 5B), which proved the extracellularly reengineering property of the nanocarrier. Additionally, the tumor growth inhibition of BALB/c mice (n = 7) bearing 4T1 tumor treated with DOX-loaded PELE/FA-DA was much better than the mice treated with the micelle that had no reengineering property or FA ligand (Fig. 5C).

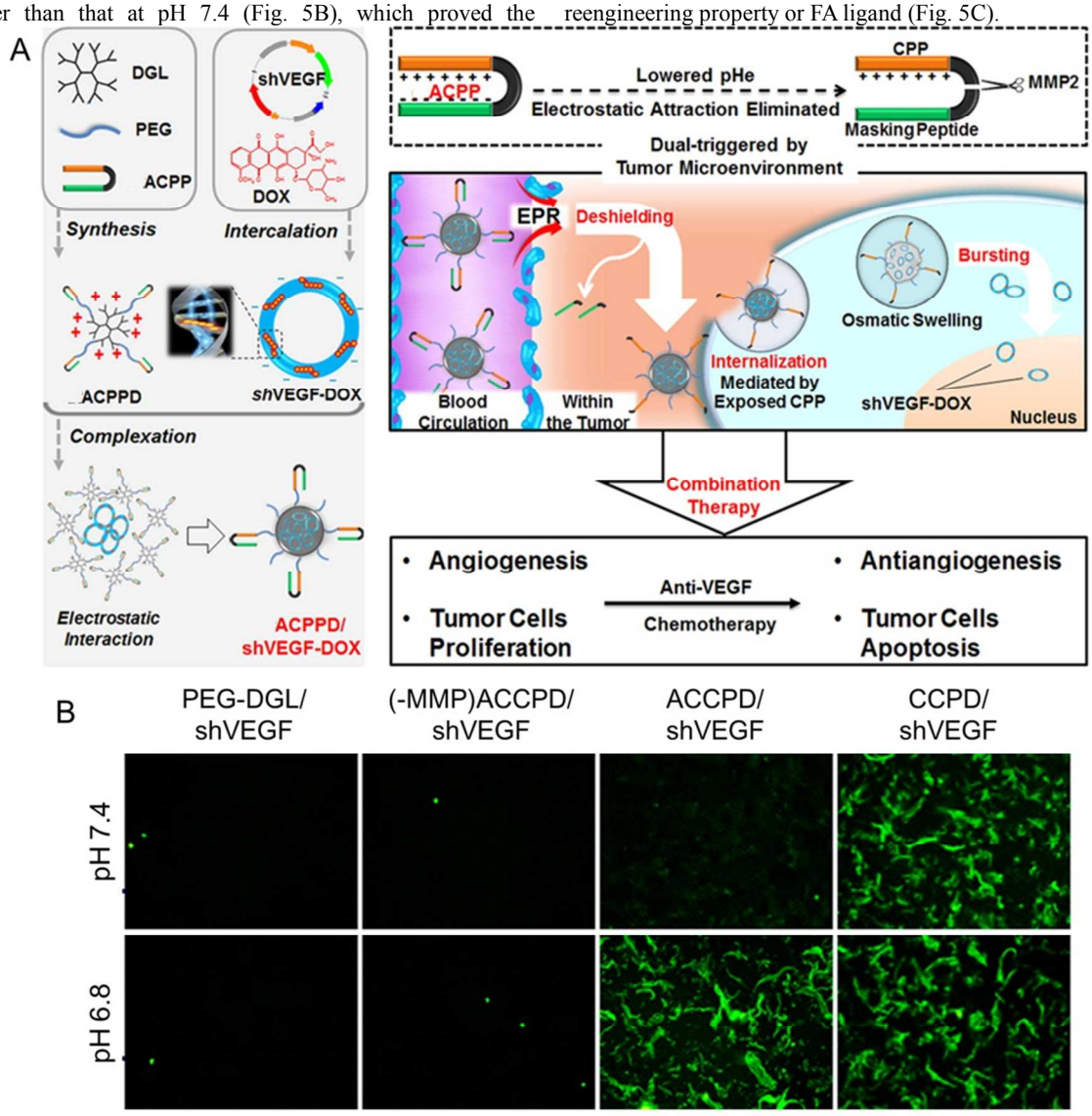

Fig. 6 (A) Construction, tumor-targeting, internalization, and combination therapy strategy of ACPP-modified nanocarrier; (B) Distribution of shVEGF in the cells treated with different formulations at pH 7.4 or 6.0. shVEGF was prelabeled by YOYO-1 (green).[64]

3.2 Enzyme-activated removal of small molecules

As introduced above, MMPs, *e.g.*, MMP-2 and MMP-9, are overexpressed in the extracellular matrix of tumor tissue, and have been widely used in the extracellular dePEGylation process.[18,47,48,62,63] Moreover, a kind of novel enzyme-sensitively activatable CPPs (ACPPs) was synthesized for the reengineering process *via* the removal of the caged small molecules.[49,59] The ACPPs were formed by two opposite charged peptides with the same length that were linked by an enzyme-cleavable linkage. During blood circulation, the negatively charged peptides were protonated and could shield the positively charged CPPs well. When the nanocarriers arrived at the tumor site, the CPPs were activated because of the departure of the negatively charged peptides resulting from the MMP-2-mediated cleavage of the enzyme-sensitive linkage and the pH-activated deprotonation of the negatively charged carboxyl groups.

Jiang's group conjugated the ACPP with a sequence of E_4K_4-x-PLGLAG-R_9-x-C to the surface of PEG-DGL, a PEG-modified G3 dendrimer with 123 lysine units, and then the ACPP-modified nanocarrier was applied to co-deliver plasmid expressing interfering RNA targeting VEGF (shVEGF) and DOX (designated as ACPPD/shVEGF-DOX) for the combination therapy of antiangiogenesis and apoptosis (Fig. 6A).[64] In detail, DOX totally intercalated into shVEGF at a molar ratio of 3:3000 (shVEGF/DOX), and ACPPD/shVEGF-DOX adopted the ratio of 6:1 (DGL/shVEGF, W/W). The nanoparticle had a narrow distribution, and the D_h was 144.9 ± 2.5 nm at pH 7.4 and 151.8 ± 2.9 nm under pH 6.0. Moreover, the corresponding zeta potential values 1.8 ± 4.1 and 3.5 ± 2.9 mV, respectively. At pH 6.0, the uptake efficiency of the MMP-2-pretreated ACPPD/shVEGF to U-87 malignant glioma cells was adequately activated (*i.e.*, 86.9%), as shown in Fig. 6B. While

without the pretreatment with MMP-2, the uptake efficiency of ACPPD/shVEGF was below 20%. Additionally, the ethidium monoazide bromide (EMA)-labeled shVEGF in ACPPD/shVEGF accumulated more in the tumor site of the glioma xenografted in nude mice than that in CPPD/shVEGF. As a result, the gene expression of ACPPD/shVEGF at the tumor site was stronger than that of CPPD/shVEGF. The apoptosis rate of the tumor in the ACPPD/shVEGF-DOX-treated group was more significant than those in the groups of control, free DOX, CPPD/shVEGF, ACPPD/DOX, and ACPPD/shVEGF. The results revealed that the excellent reengineering capability improved the property of the above nanocarrier.

Similarly, ACPP with a more simple sequence of R_8-PLGLAG-E_8 was applied to modify the nanocarrier to overcome the blood-brain barrier and blood-tumor barrier in the treatment of glioma.[65] The nanocarrier self-assembled from PEG-*b*-PCL was dual-modified with ACPP and angiopep-2. The hydrodynamic size was 115.3 nm with PDI of 0.228, and the zeta potential was –6.72 mV. DTX was loaded into the micelle. The modification of both ACPP and CPP increased the cell uptake of the MMP-2-overexpressed BMEC brain microvessel endothelial cells and C6 glioma cells (from rat). The cell internalization of the ACPP-modified nanocarrier was inhibited by batimastat, an MMP-2 inhibitor, suggesting that the cell-penetrating property of ACPP could be activated by MMP-2. The glioma-bearing mouse treated with ACPP and angiopep-2 dual-modified nanocarrier loading with DiR showed higher fluorescence intensity at tumor site compared with the mouse treated with the unmodified, angiopep-2-modified, ACPP-modified, or CPP-modified one, which was mainly because of the combination of the ACPP-mediated extracellularly reengineering and the angiopep-2-mediated tumor targeting. Finally, the DTX-loaded dual-modified nanocarrier exhibited the prolonged survival time than the non-modified or single-modified one. As a result, the tumor site activatable ACPP-functionalized nanoparticle may have great potential in the treatment of glioma.

3.3 Light-triggered uncaging process

As introduced before, light has been widely applied in the PEG-detachable nanocarriers, which usually had photo-cleavable linkages between the PEG block and the hydrophobic block for extracellularly dePEGylation. Additionally, the photo-sensitive groups could also been used to cage the ligands on the surface of nanocarriers.[21,49,66–68] Ashkenasy, David, and coworkers presented the modification of CPP on the surface of nanoparticle by the photo-cleavable small molecule.[49] In detail, the caged CPP was prepared by temporarily caging the lysine groups on the peptide of ^{52}RRMKWKK^{58} with 6-nitroveratrylcarbonyl (Nvoc). Once being treated by the illumination of UV light (λ = 365 nm) for 10 min, the caging Nvoc was removed, and the cell transduction activity of CPP was subsequently restored. The cell uptake to PC-3 cells (a human prostate carcinoma cell line) under illumination of 10 min was enhanced compared with that without irradiation. In addition, a proapoptotic peptide, *i.e.*, $_D$(KLAKLAK)$_2$, was conjugated to the side chain of the ACPP-modified *N*-(2-hydroxypropyl) methacrylamide (HPMA) through a pH-sensitive hydrazone bond. The cytotoxicity of the proapoptotic peptide-conjugated copolymer to PC-3 cells increased along with the illumination with UV light.

Yeh and coworkers have contributed a lot to the development of the *o*-nitrobenzyl-caged FA through covalently binding to α- and γ-carboxylate groups, which interacted with folate receptors (FRs) on the cell surface.[66,67] As a typical example, the PLGA@lipid nanocarriers were firstly prepared by the self-assembly of PLGA, 1,2-dipalmitoyl-*sn*-glycero-3-phosphocholine (DPPC), and 1,2-distearoyl-*sn*-glycero-3-phosphoethanolamine-*N*-[carboxy poly(ethylene glycol)2000] (DSPE-cPEG2000) *via* a single-step nanoprecipitation approach.[66] Then FA was anchored on the surface of PLGA@lipid to form the FA/PLGA@lipid nanoconjugate. At last, the anchored FA was caged by the 2-nitrobenzylamine (NBA) to form the caged FA/PLGA@lipid nanocarrier with average D_h and zeta potential at 173 nm and –28.3 mV, respectively, for photo-controlled reengineering. The NBA-caged FA/PLGA@lipid nanocarrier loading PTX with DLC of 0.17 wt.% showed low cytotoxicity toward KB cells (a human oral epithelial carcinoma cell line) without irradiation. However, when co-cultured with cells under irradiation for 20 min, the formulation showed the similar inhibition capability against KB cells in relation to that of FA/PLGA@lipid. The result indicated the successful cytotoxicity decrease toward the normal tissue and the activatable antitumor efficacy after the light-mediated reengineering process.

4 Other shell-sheddable polymer-free platforms and emerging mechanisms

Additionally, there are some other drug delivery systems that have the reengineered property but should not be belonged to the polymeric nanocarriers, such as liposome,[62,66,69] and mesoporous silica,[70] magnetic,[71] quantum dot,[72] gold,[73] and upconversion nanoparticles.[67] In addition, the non-polymeric platforms show remarkable synergistic therapeutic potential in the combination of chemotherapy and other treatment modalities with different mechanisms. For instance, the ultrathin silica-coated nanocarrier with D_h of ~200 nm was prepared by Chen and coworkers for the combination of chemotherapy and ablation by high-intensity focused ultrasound.[74] The silica coating could be broken under ultrasound, and the loaded camptothecin (CPT) was released at the tumor side for directional drug delivery.

Furthermore, some novel reengineered approaches have emerged, such as polymer-caged[75,76] and "pop-up" strategies.[68,77,78] In Zhou and Gu's group, an enzymatically degradable hyaluronic acid (HA) modified with acrylated pendants was used to encapsulate the DOX-loaded and CPP (*i.e.*, R8H3)-modified liposome (*i.e.*, DOX-Gelipo).[76] In addition, tumor necrosis factor-related apoptosis inducing ligand (TRAIL), which acted on the death receptor (DR) on the plasma membrane, was encapsulated in the outer shell made of crosslinked HA yielding TRAIL-Gelipo. The notably increased D_h of 120 nm and a highly negative surface charge of –22 mV indicated the successful coating of the HA-crosslinked gel shell on the surface of the liposomal core. The crosslinked polymer cage could be degraded by hyaluronidase (HAase), and then the TRAIL and DOX-loaded liposome were released to the tumor extracellular matrix for both antitumor activity and enhanced cell uptake. After incubation with HAase for 1 h, the D_h of the nanoparticle reduced sharply from 125 nm to 83 nm, and the surface charge reversed from –20 to 10 mV, suggesting that the enzyme-sensitive degradation of the shell, and the exposure of positive charge. The rhodamine-labeled TRAIL (r-TRAIL) was distributed on the cells membrane of MDA-MB-231 cells incubated with r-TRAIL-Gelipo pretreated with HAase for 1 h at 37 °C to trigger the following extrinsic apoptosis pathway, while the non-pretreated nanoparticle was distributed into the cells resulting from the endocytosis of whole nanocarrier. Moreover, the intracellular delivery of DOX from the HAase-pretreated nanoparticle toward MDA-MB-231 cells increased as time. The TRAIL and DOX co-loaded nanocarrier showed enhanced antitumor activity to the MDA-MB-231 tumor-bearing nude mice compared with free DOX and DOX-loaded nanocarrier. In addition, Bae's group declared another reengineered approach through "pop-up" strategy.[77] The polymeric micelle system with TAT peptide on its surface exhibited a D_h of ~95 nm and could response to a small

change of pH. At above pH 7.0, TAT peptide was anchored on the hydrophobic core because of the hydrophobic short linkage of PLH between the PEG block and TAT peptide. When the condition became slightly acidic (pH ~6.5 – 7.0), the PLH block became charged and exposed the TAT peptide to the outside of PEG shell. The cell uptake of the FITC-labeled "pop-up" nanocarrier increased as the decrease of pH. The DOX-loaded nanocarrier modified with "pop-up" TAT peptide showed increased inhibition of MCF-7 cells when the pH decreased below 7.0. The similar result was found in the drug-resistant tumor cells, such as NCI/ADR-RES cells (P-glycoprotein-overexpressed human ovarian tumor cell line), NCI-H69/AR cells (multidrug resistance protein-overexpressed human ovarian tumor cell line), HL-60 cells (Bcl-2 protein-overexpressed human promyelocytic leukemia cell line), HL-60/MX2 cells (altered Topo II-expressed human promyelocytic leukemia cell line), and A549 cells (lung resistance protein-overexpressed human lung tumor cell line), which proved the efficient inhibition of drug-resistant tumor cells. Additionally, the DOX-loaded "pop-up" nanoparticle also showed enhanced tumor inhibition in the MCF-7, A2780/AD (a human ovarian), or A549 tumor bearing nude mice than the free DOX and nanoparticle without modification or modified with "non-pop-up" TAT peptide.

5 Conclusions and perspectives

The extracellularly reengineered polymeric nanocarriers in tumor tissue integrate the prolonged blood circulation and enhanced cell uptake in one single system. With PEGylation or small molecule cage, the nanocarriers remain stability and stealthy in the blood circulation. When they accumulate into the tumor tissue, the shielded PEG or small molecules are removed under the extracellular stimuli, which reactivate their ability of enhancing endocytosis. The property improves their antitumor efficacy, especially toward the drug resistant-tumors[34,60] or gliomas[64,65] that hide behind the blood-brain barrier. In this review, we highlight several representatives of the tumor extracellular stimuli-responsive polymeric nanocarriers. The pH- and enzyme-dependent reengineering processes are most popularly used because of their universality in most kinds of tumors. But it is worth noting that the pH difference between blood and tumor tissue or the enzyme concentration difference between normal and tumor tissue are not obviously. As a result, the external stimuli are necessary for the accurate reengineering processes. The position and intensity of the external stimuli are easy to be adjusted according to different cases. Perhaps, the combination of the internal and external stimuli is possible for a better tumor targeting efficiency.[79]

For the systemic administration of ideal drug delivery systems in chemotherapy, the integral drug delivery cascade have been summarized and must include the following five features: (i) prolonged circulation time, (ii) enhanced tumor accumulation, (iii) promoted tumor penetration, (iv) increased cell uptake, and (v) accelerated intracellular drug release. It is demonstrated that the extracellularly reengineered polymeric nanocarriers highlighted in this review play an important role in the entire process of drug delivery and will be guidelines for the next generation of drug nanocarriers.

Acknowledgements

This work was financially supported by the National Natural Science Foundation of China (Projects 51303174, 51233004, 51390484, 51321062, 51273196, and 51203153) and the Scientific Development Program of Jilin Province (Project 20140520050JH and 20130206058GX).

Notes and references

[a] *Key Laboratory of Polymer Ecomaterials, Changchun Institute of Applied Chemistry, Chinese Academy of Sciences, Changchun 130022, P. R. China. E-mail: jxding@ciac.ac.cn; xschen@ciac.ac.cn; Fax: +86 431 85262116; Tel: +86 431 85262116*

[b] *University of Chinese Academy of Sciences, Beijing 100049, P. R. China*

1 J. X. Ding, J. J. Chen, D. Li, C. S. Xiao, J. C. Zhang, C. L. He, X. L. Zhuang and X. S. Chen, *J. Mater. Chem. B*, 2013, **1**, 69–81.

2 Z. Yuan, D. Zhao, X. Yi, R. Zhuo and F. Li, *Adv. Funct. Mater.*, 2014, **24**, 1799–1807.

3 Z. He, B. Chu, X. Wei, J. Li, E. Carl, X. Song, G. He, Y. Xie, Y. Wei and Z. Qian, *Int. J. Pharm.*, 2014, **469**, 168–178.

4 Y. Huang, Y. Jiang, H. Wang, J. Wang, M. C. Shin, Y. Byun, H. He, Y. Liang and V. C. Yang, *Adv. Drug Deliver. Rev.*, 2013, **65**, 1299–1315.

5 B. Romberg, W. E. Hennink and G. Storm, *Pharm. Res.*, 2008, **25**, 55–71.

6 M. C. Woodle, C. M. Engbers and S. Zalipsky, *Bioconjugate Chem.*, 1994, **5**, 493–496.

7 J. Fang, H. Nakamura and H. Maeda, *Adv. Drug Deliver. Rev.*, 2011, **63**, 136–151.

8 J. Lee, J. Kim, K. Bae, M. Oh, Y. Kim, J. Kim, T. Park, K. Park, J. Lee and Y. Nam, *Small*, 2015, **11**, 222–231.

9 G. Fontana, M. Licciardi, S. Mansueto, D. Schillaci and G. Giammona, *Biomaterials*, 2001, **22**, 2857–2865.

10 Q. Sun, X. Sun, X. Ma, Z. Zhou, E. Jin, B. Zhang, Y. Shen, E. A. Van Kirk, W. J. Murdoch, J. R. Lott, T. P. Lodge, M. Radosz and Y. Zhao, *Adv. Mater.*, 2014, **26**, 7615–7621.

11 R. Cheng, F. Meng, C. Deng, H. A. Klok and Z. Zhong, *Biomaterials*, 2013, **34**, 3647–3657.

12 J. Z. Du, C. Q. Mao, Y. Y. Yuan, X. Z. Yang and J. Wang, *Biotechnol. Adv.*, 2014, **32**, 789–803.

13 E. Gullotti and Y. Yeo, *Mol. Pharm.*, 2009, **6**, 1041–1051.

14 E. S. Lee, Z. Gao and Y. H. Bae, *J. Control. Release*, 2008, **132**, 164–170.

15 S. Binauld and M. H. Stenzel, *Chem. Commun.*, 2013, **49**, 2082–2102.

16 J. X. Ding, L. H. Chen, C. S. Xiao, L. Chen, X. L. Zhuang and X. S. Chen, *Chem. Commun.*, 2014, **50**, 11274–11290.

17 J. X. Gu, W. P. Cheng, J. G. Liu, S. Y. Lo, D. Smith, X. Z. Qu and Z. Z. Yang, *Biomacromolecules*, 2008, **9**, 255–262.

18 P. S. Kulkarni, M. K. Haldar, R. R. Nahire, P. Katti, A. H. Ambre, W. W. Muhonen, J. B. Shabb, S. K. R. Padi, R. K. Singh, P. P. Borowicz, D. K. Shrivastava, K. S. Katti, K. Reindl, B. Guo and S. Mallik, *Mol. Pharm.*, 2014, **11**, 2390–2399.

19 J. Z. Du, T. M. Sun, W. J. Song, J. Wu and J. Wang, *Angew. Chem., Int. Edit.*, 2010, **122**, 3703–3708.

20 P. Xu, E. A. Van Kirk, Y. Zhan, W. J. Murdoch, M. Radosz and Y. Shen, *Angew. Chem., Int. Edit.*, 2007, **46**, 4999–5002.

21 T. Dvir, M. R. Banghart, B. P. Timko, R. Langer and D. S. Kohane, *Nano Lett.*, 2009, **10**, 250–254.

22 E. C. Cho, J. W. Xie, P. A. Wurm and Y. N. Xia, *Nano Lett.*, 2009, **9**, 1080–1084.

23 L. Tian and Y. H. Bae, *Colloid Surf. B, Biointerfaces*, 2012, **99**, 116–126.

24 S. D. Li and L. Huang, *J. Control. Release*, 2010, **145**, 178–181.

25 F. M. Veronese and G. Pasut, *Drug Discov. Today*, 2005, **10**, 1451–1458.

26 F. Q. Hu, Y. Y. Zhang, J. You, H. Yuan and Y. Z. Du, *Mol. Pharm*. 2012, **9**, 2469–2478.
27 J. Rao and A. Khan, *J. Am. Chem. Soc*., 2013, **135**, 14056–14059.
28 J. S. Katz, S. Zhong, B. G. Ricart, D. J. Pochan, D. A. Hammer and J. A. Burdick, *J. Am. Chem. Soc*., 2010, **132**, 3654–3655.
29 J. M. Schumers, J. F. Gohy and C. A. Fustin, *Polym. Chem*., 2010, **1**, 161–163.
30 H. Yang, L. Jia, Z. Wang, A. L. Di Cicco, D. Lévy and P. Keller, *Macromolecules*, 2010, **44**, 159–165.
31 M. Rabnawaz and G. Liu, *Macromolecules*, 2012, **45**, 5586–5595.
32 L. Peng, A. Feng, H. Zhang, H. Wang, C. Jian, B. Liu, W. Gao and J. Yuan, *Polym. Chem*., 2014, **5**, 1751–1759.
33 V. A. Sethuraman and Y. H. Bae, *J. Control. Release*, 2007, **118**, 216–224.
34 X. Z. Yang, X. J. Du, Y. Liu, Y. H. Zhu, Y. Z. Liu, Y. P. Li and J. Wang, *Adv. Mater*., 2014, **26**, 931–936.
35 X. Ma and Y. Zhao, *Chem. Rev*., 2014, DOI: 10.1021/cr500392w.
36 G. Yu, C. Han, Z. Zhang, J. Chen, X. Yan, B. Zheng, S. Liu and F. Huang, *J. Am. Chem. Soc*., 2012, **134**, 8711–8717.
37 A. C. Feng, Q. Yan, H. J. Zhang, L. Peng and J. Y. Yuan, *Chem. Commun.*, 2014, **50**, 4740–4742.
38 J. Ding, W. Xu, Y. Zhang, D. Sun, C. Xiao, D. Liu, X. Zhu and X. Chen, *J. Control. Release*, 2013, **172**, 444–455.
39 J. J. Chen, J. X. Ding, Y. Zhang, C. S. Xiao, X. L. Zhuang and X. S. Chen, *Polym. Chem*., 2015, **6**, 397–405.
40 F. Meng, Y. Zhong, R. Cheng, C. Deng and Z. Zhong, *Nanomedicine*, 2014, **9**, 487–499.
41 Z. Zhou, Y. Shen, J. Tang, M. Fan, E. A. Van Kirk, W. J. Murdoch and M. Radosz, *Adv. Funct. Mater*., 2009, **19**, 3580–3589.
42 C. Ding, J. Gu, X. Qu and Z. Yang, *Bioconjugate Chem*., 2009, **20**, 1163–1170.
43 N. Song, M. Ding, Z. Pan, J. Li, L. Zhou, H. Tan and Q. Fu, *Biomacromolecules*, 2013, **14**, 4407–4419.
44 J. Hu, S. Miura, K. Na and Y. H. Bae, *J. Control. Release*, 2013, **172**, 69–76.
45 M. Egeblad and Z. Werb, *Nat. Rev. Cancer*, 2002, **2**, 161–174.
46 R. de la Rica, D. Aili and M. M. Stevens, *Adv. Drug Deliver. Rev*., 2012, **64**, 967–978.
47 F. B. Cui, R. T. Li, Q. Liu, P. y. Wu, W. j. Hu, G. f. Yue, H. Ding, L. X. Yu, X. P. Qian and B. R. Liu, *Cancer Lett*., 2014, **346**, 53–62.
48 E. Gullotti, J. Park and Y. Yeo, *Pharm. Res*., 2013, **30**, 1956–1967.
49 Y. Shamay, L. Adar, G. Ashkenasy and A. David, *Biomaterials*, 2011, **32**, 1377–1386.
50 R. Tong, H. D. Hemmati, R. Langer and D. S. Kohane, *J. Am. Chem. Soc*., 2012, **134**, 8848–8855.
51 J. F. Gohy and Y. Zhao, *Chem. Soc. Rev*., 2013, **42**, 7117–7129.
52 G. Liu, W. Liu and C. M. Dong, *Polym. Chem*., 2013, **4**, 3431–3443.
53 L. Peng, A. Feng, M. Huo and J. Yuan, *Chem. Commun.*, 2014, **50**, 13005–13014.
54 Q. Yan, J. Y. Yuan, Z. N. Cai, Y. Xin, Y. Kang and Y. W. Yin, *J. Am. Chem. Soc*., 2010, **132**, 9268–9270.
55 Q. Yan, A. Feng, H. Zhang, Y. Yin and J. Yuan, *Polym. Chem*., 2013, **4**, 1216–1220.
56 N. Q. Shi, X. R. Qi, B. Xiang and Y. Zhang, *J. Control. Release*, 2014, **194**, 53–70.
57 J. Li, Y. Han, Q. Chen, H. Shi, S. ur Rehman, M. Siddiq, Z. Ge and S. Liu, *J. Mater. Chem. B*, 2014, **2**, 1813–1824.
58 H. Huang, Y. Li, Z. Sa, Y. Sun, Y. Wang and J. Wang, *Macromol. Biosci*., 2014, **14**, 485–490.
59 W. Gao, B. Xiang, T. T. Meng, F. Liu and X. R. Qi, *Biomaterials*, 2013, **34**, 4137–4149.
60 J. Z. Du, X. J. Du, C. Q. Mao and J. Wang, *J. Am. Chem. Soc*., 2011, **133**, 17560–17563.
61 X. Guo, C. Shi, G. Yang, J. Wang, Z. Cai and S. Zhou, *Chem. Mater*., 2014, **26**, 4405–4418.
62 L. Zhu, P. Kate and V. P. Torchilin, *ACS Nano*, 2012, **6**, 3491–3498.
63 Y. Wan, J. Han, G. Fan, Z. Zhang, T. Gong and X. Sun, *Biomaterials*, 2013, **34**, 3020–3030.
64 S. Huang, K. Shao, Y. Liu, Y. Kuang, J. Li, S. An, Y. Guo, H. Ma and C. Jiang, *ACS Nano*, 2013, **7**, 2860–2871.
65 H. Gao, S. Zhang, S. Cao, Z. Yang, Z. Pang and X. Jiang, *Mol. Pharm*., 2014, **11**, 2755–2763.
66 N. C. Fan, F. Y. Cheng, J. A. A. Ho and C. S. Yeh, *Angew. Chem., Int. Edit*., 2012, **51**, 8806–8810.
67 Y. H. Chien, Y. L. Chou, S. W. Wang, S. T. Hung, M. C. Liau, Y. J. Chao, C. H. Su and C. S. Yeh, *ACS Nano*, 2013, **7**, 8516–8528.
68 M. B. Hansen, E. van Gaal, I. Minten, G. Storm, J. C. M. van Hest and D. W. P. M. Löwik, *J. Control. Release*, 2012, **164**, 87–94.
69 Y. T. Chiang and C. L. Lo, *Biomaterials*, 2014, **35**, 5414–5424.
70 B. Chang, D. Chen, Y. Wang, Y. Chen, Y. Jiao, X. Sha and W. Yang, *Chem. Mater*., 2013, **25**, 574–585.
71 J. Wang, C. Gong, Y. Wang and G. Wu, *Colloid Surf. B, Biointerfaces*, 2014, **118**, 218–225.
72 S. B. Lowe, J. A. G. Dick, B. E. Cohen and M. M. Stevens, *ACS Nano*, 2011, **6**, 851–857.
73 S. Rana, A. Bajaj, R. Mout and V. M. Rotello, *Adv. Drug Deliver. Rev*., 2012, **64**, 200–216.
74 M. Ma, H. Xu, H. Chen, X. Jia, K. Zhang, Q. Wang, S. Zheng, R. Wu, M. Yao, X. Cai, F. Li and J. Shi, *Adv. Mater*., 2014, **26**, 7378–7385.
75 M. T. Basel, T. B. Shrestha, D. L. Troyer and S. H. Bossmann, *ACS Nano*, 2011, **5**, 2162–2175.
76 T. Jiang, R. Mo, A. Bellotti, J. Zhou and Z. Gu, *Adv. Funct. Mater*., 2014, **24**, 2295–2304.
77 E. S. Lee, Z. Gao, D. Kim, K. Park, I. C. Kwon and Y. H. Bae, *J. Control. Release*, 2008, **129**, 228–236.
78 Z. Yuan, Z. Que, S. Cheng, R. Zhuo and F. Li, *Chem. Commun.*, 2012, **48**, 8129–8131.
79 J. Xuan, D. Han, H. Xia and Y. Zhao, *Langmuir*, 2013, **30**, 410–417.

Colour TOC Graphic

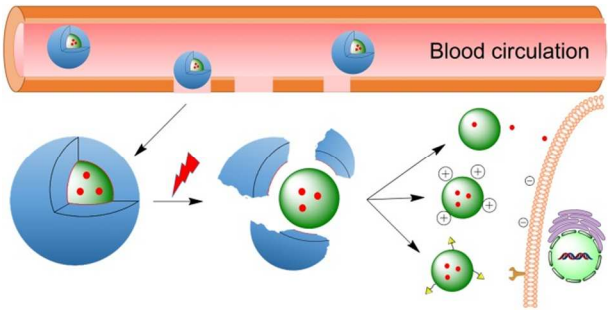

Text

The review gives the comprehensive summary and preliminary forecast of the extracellularly stimuli-mediated shell-sheddable polymeric nanocarriers for antitumor applications.

Photographs and biographies

Jinjin Chen

Jinjin Chen received his BS degree from University of Science and Technology of China (USTC) in 2012. He is now studying for his PhD degree under the supervision of *Prof.* Xuesi Chen in Key Laboratory of Polymer Ecomaterials (KLPE), Changchun Institute of Applied Chemistry (CIAC), Chinese Academy of Sciences (CAS). His research interests are focused on designs and preparations of intelligent platforms for controlled antitumor drug delivery.

Jianxun Ding

Jianxun Ding is currently an assistant professor in KLPE, CIAC, CAS. He received his BS degree from USTC in 2007, and obtained his PhD degree in CIAC, CAS in 2013 under the supervision of *Prof.* Xuesi Chen. During the PhD, he was awarded 2012 President Excellence Award of CAS. He has published more than 60 academic papers with h-index of 16 and applied over 50 Chinese invention patents. His research focuses on (1) exploitations of biodegradable stimuli-responsive polymers as the matrices of smart nanocarriers, and (2) developments of cell-related nanoscale platforms for controlled drug delivery.

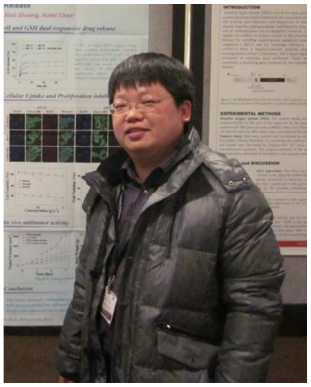

Chunsheng Xiao

Chunsheng Xiao is now an associate professor in KLPE, CIAC, CAS. He received his PhD degree from CIAC, CAS in 2011 under the supervision of *Prof.* Xuesi Chen. He has authored/coauthored more than 50 research papers with h-index of 16. His currently research interests include designs and syntheses of stimuli-responsive polyesters and polypeptides for biomedical applications.

Xiuli Zhuang

Xiuli Zhuang has been a professor in CIAC, CAS since 2011. She graduated from CIAC, CAS and received her MS degree in 1994, and earned her PhD degree in Waseda University, Japan, in 2010. Up to now, she has published more than 120 pre-reviewed research papers. In addition, she has applied over 120 Chinese patents, of which more than 70 ones were authorized. Recently, her research focuses on developments of (1) industrializations of biodegradable polymers (*e.g.*, polylactide, poly(lactide-*co*-glycolide), and polypeptides) as biomaterials, and (2) stimuli-responsive biodegradable polymeric nanoparticles for controlled drug delivery.

Xuesi Chen

Xuesi Chen received his PhD degree at Waseda University, Japan, in 1997, and completed his post-doctoral fellowship at University of Pennsylvania, USA, in 1999. He has been a full Professor at CIAC, CAS since 1999. He has published over 500 articles in academic journals, which have been cited for more than 9,000 times until now. In addition, he has applied over 250 Chinese patents and more than 120 ones have been authorized. His research interests focus on preparations and biomedical applications of biodegradable polymers, mainly focused on polyethers, polyesters, polypeptides, polycarbonates, and their copolymers.